

CONF-730728--1

DESIGN AND CONSTRUCTION OF A LOW VELOCITY  
BOUNDARY-LAYER TEMPERATURE PROBE<sup>†</sup>

SLA - 73 - 5604

Ben F. Blackwell<sup>\*</sup>

Sandia Laboratories, Albuquerque, New Mexico 87115

R. J. Moffat<sup>‡</sup>

Stanford University, Stanford, California 94305

Abstract

A small thermocouple temperature probe has been designed and fabricated for use in low velocity turbulent boundary-layer studies. The primary probe design objective was the elimination of temperature errors due to conduction along the thermoelectric elements. It is shown that not only probe geometry but also the thermal characteristics of the two thermoelectric elements influence conduction errors. Design curves for four common thermoelectric pairs are presented. An experimental turbulent boundary-layer temperature profile is presented and compared with the theoretical laminar sub-layer equation to verify that the designed probe was free of conduction errors.

<sup>†</sup> This work was supported by NASA Grant NGL 05-020-134. Additionally, the work of the first author was supported by the U. S. Atomic Energy Commission.

<sup>\*</sup> Member, Technical Staff, Reentry Vehicle Aerothermodynamics Division.

<sup>‡</sup> Director, Thermosciences Division, Mechanical Engineering Department.

—NOTICE—

This report was prepared as an account of work sponsored by the United States Government. Neither the United States nor the United States Atomic Energy Commission, nor any of their employees, nor any of their contractors, subcontractors, or their employees, makes any warranty, express or implied, or assumes any legal liability or responsibility for the accuracy, completeness or usefulness of any information, apparatus, product or process disclosed, or represents that its use would not infringe privately owned rights.

MASTER

## Design and Construction of a Low Velocity

### Boundary-Layer Temperature Probe

When a temperature-sensing instrument such as a thermocouple is immersed in a fluid, the indicated temperature will usually differ from the true temperature of the undisturbed fluid, even if the presence of the sensor does not alter the flow field. Heat conduction along the thermoelectric wires is a common source of thermocouple error, and can be particularly severe in the small probes used in turbulent boundary-layers because the sensing element must operate in regions of very steep temperature gradients. In this Note, it is shown that conduction errors can be kept within acceptable limits by the proper choice of thermoelectric pair and/or probe geometry, and that turbulent boundary-layer temperature profiles can be measured accurately.

In the experimental turbulent boundary-layer study of Blackwell, Kays, and Moffat<sup>1</sup>, it was desired to measure mean temperature profiles inside the logarithmic portion of the boundary-layer to determine the turbulent Prandtl number in this region. This made it necessary that the probe be very small, since this region may be only a few thousandths of an inch in extent. The basic probe configuration chosen was a thermocouple with the two wires of equal diameter, and the junction formed by butt welding. A schematic of the probe is shown in Fig. 1.

The geometrical characteristics ( $L_1$ ,  $L_2$ ,  $D$ ) and thermal conductivity ( $k_1$ ,  $k_2$ ) of the thermoelectric elements were chosen with the intent that heat conduction errors would be below an acceptable level. This

was accomplished by analyzing the probe as a one-dimensional fin with convection from the surface and a specified (and equal) temperature at the two ends. From the analysis of Davis<sup>2</sup> or Blackwell, et al<sup>1</sup>, it can be shown that the nondimensional junction temperature can be expressed as

$$\theta_j = \frac{T_j - T_f}{T_o - T_f} = \frac{\kappa \sinh(\kappa p_2) + \sinh(p_2)}{\kappa \sinh(\kappa p_2) \cosh(p_2) + \sinh(p_2) \cosh(\kappa p_2)} \quad (1)$$

where the fin parameters are defined by

$$p_{1,2} = 2 \sqrt{\frac{hD}{k_{1,2}}} \frac{L_{1,2}}{D}, \quad (2)$$

$$\kappa = \frac{p_1}{p_2} = \sqrt{\frac{k_2}{k_1} \frac{L_1}{L_2}}, \quad (3)$$

and  $h$  is the convective heat transfer coefficient. All temperatures in Eq. 1 are defined with the aid of Fig. 1. Figure 2 presents the nondimensional junction temperature as a function of  $\kappa$ , with  $p_2$  as a parameter. Note that for a given value of  $p_2$ , there is an optimum value of  $\kappa$  that corresponds to a minimum  $\theta_j$ . Any additional increase in  $\kappa$  causes a decrease in probe performance. As  $p_2$  becomes large, the optimum value of  $\kappa$  approaches unity. For each value of  $p_2$  the curves approach the adiabatic fin solution,  $\theta_j = \frac{1}{\cosh p_2}$ , as  $\kappa$  goes to infinity. Intermediate values of  $\kappa$  result in lower values of  $\theta$  because

part of fin 1 acts as an effective extension of fin 2. Low values of  $\kappa$  show increasing error (increasing  $\theta_j$ ) by thermally connecting the junction to the support.

Up to this point in the analysis, it has been assumed that  $\kappa$  can take on a continuous range of values. Since only certain materials ( $k_1, k_2$ ) are desirable in a thermocouple, the continuous property of  $\kappa$  depends on whether the length ratio  $L_2/L_1$  can assume a continuous range of values (see Eq. 3). In some applications, it might be desirable to specify  $L_2/L_1$  on some basis other than the elimination of conduction errors. For example, the thermocouple junction should be located as far as possible from either probe support to eliminate interference problems. For this situation, one might choose  $L_2/L_1$  approximately unity. In this case,  $\kappa$  becomes a discrete parameter that depends only on the thermal conductivity of the two thermoelectric materials.

If we restrict the analysis to some of the more common thermocouple materials, the data in Fig. 2 can be put in a much more useful form. Figure 3a presents the thermocouple junction temperature as a function of the fin parameter  $p_2$  for three thermocouples, each with constantan as the negative element. The thermal conductivity values used are presented in Table 1. The subscripts 1 and 2 refer to the first- and second-named elements of the thermocouple respectively. Of the three thermocouples in Fig. 3a, chromel-constantan is the best from the standpoint of conduction losses. In fact, copper-constantan would require an aspect ratio ( $L/D$ ) approximately four times that of

chromel-constantan if the same value of nondimensional junction temperature  $\theta_j$  were to be maintained.

In Fig. 3b, a chromel-alumel probe is compared with a chromel-constantan probe. Since chromel ( $k_1$ ) is common to both,  $\theta_j$  is presented as a function of  $p_1$ , allowing a more direct comparison of the two thermocouple pairs. From this data, the chromel-constantan probe will require a smaller aspect ratio ( $L/D$ ) if a given value of junction temperature is to be maintained.

On the basis of the information given in the above discussion, the thermocouple material selected was chromel-constantan.\*  
Commercially available 0.003-inch (0.076-mm)-diameter thermocouple wire with a Teflon insulator was butt-welded to form the thermocouple junction. After welding, the thermocouple was rolled between two pieces of flat steel to remove kinks. The sensing element was supported between two 22-gauge stainless-steel hypodermic needles, with the Teflon providing electrical isolation between the thermocouple wire and the stainless steel. The Teflon insulator was burned off the part of the thermocouple that was exposed to the gas stream. Contact between the bare thermocouple wire and the hypodermic needle occurred only at the end of the needle. Since the two needles were electrically insulated from each other, this contact did not form a closed loop that would introduce an additional emf. The

---

\* Additionally, the chromel-constantan combination has the steepest emf-versus-temperature relationship of the four thermocouples considered in this Note.

hypodermic needles were shaped to give some spring to the probe assembly when in contact with the wall. A completed probe assembly is shown in Fig. 4.

The probe span ( $L$ ) was chosen with the aid of the design curves in Fig. 3. It was estimated that the minimum velocity to be encountered in the laminar sublayer (in air) would be approximately 2 ft/sec (0.6 m/sec), and it was desired to keep the dimensionless junction temperature  $\theta_j$  below 0.005. The data in Fig. 3 indicates that a span of 0.5 inch (1.27 cm) is adequate to satisfy the above condition on  $\theta_j$  for a chromel-constantan probe.

Figure 5 presents a typical turbulent boundary-layer temperature profile (in wall coordinates) taken from the study of Blackwell, et al<sup>1</sup>. Also shown is the theoretical laminar sublayer equation  $T^+ = Pr y^+$ . Agreement between the laminar sublayer equation and experiment is excellent. It is more difficult to make accurate temperature measurements in the laminar sublayer than in any other region of the boundary layer. The fact that experimental data and theory agree in this region indicates that the probe was essentially free of conduction errors.

In summary, chromel-constantan is the best, from the standpoint of conduction losses, of the four thermocouples considered in this study, provided the junction is located in the center of the span.

### References

1. Blackwell, B. F., Kays, W. M., and Moffat, R. J., "The Turbulent Boundary Layer on a Porous Plate: An Experimental Study of the Heat Transfer Behavior with Adverse Pressure Gradients," HMT-16, August 1972, Thermosciences Division, Mechanical Engineering Department, Stanford University, Stanford, California.
2. Davis, M. R., "General Response of Resistance Thermometers and Thermocouples in Gases at Low Pressure," AIAA Journal, Vol. 10, No. 4, April 1972, pp. 546-547.
3. Benedict, R. P., Fundamentals of Temperature, Pressure, and Flow Measurements, Wiley, New York, 1969, p. 151.

TABLE 1

Thermal Conductivity Data (From Benedict<sup>3</sup>)

<u>Thermoelectric Element</u>	<u>k, Btu/Ft-Sec-°F</u>
Copper	0.0616
Iron	0.0096
Alumel	0.0048
Constantan	0.0038
Chromel	0.0031



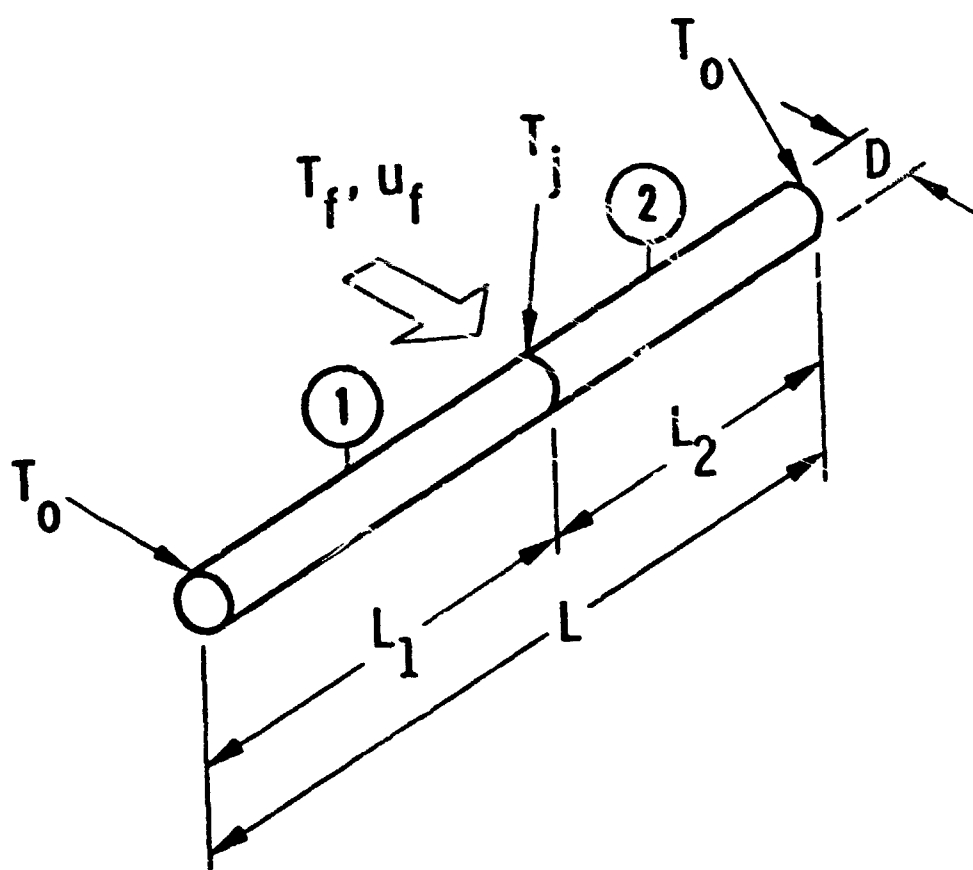


Figure 1. Schematic of boundary-layer probe.

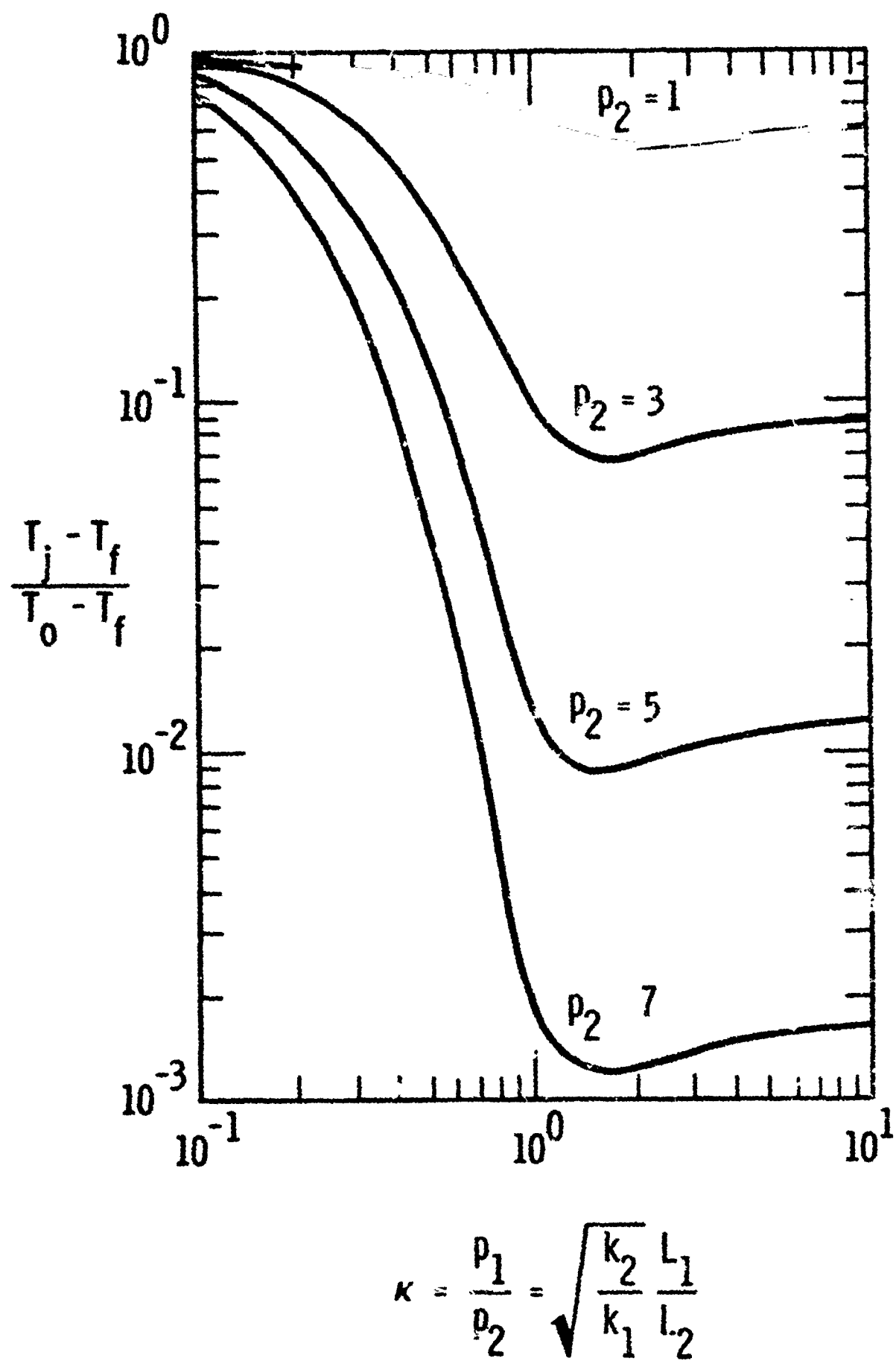


Figure 2. Dimensionless junction temperature for various values of the fin parameters.

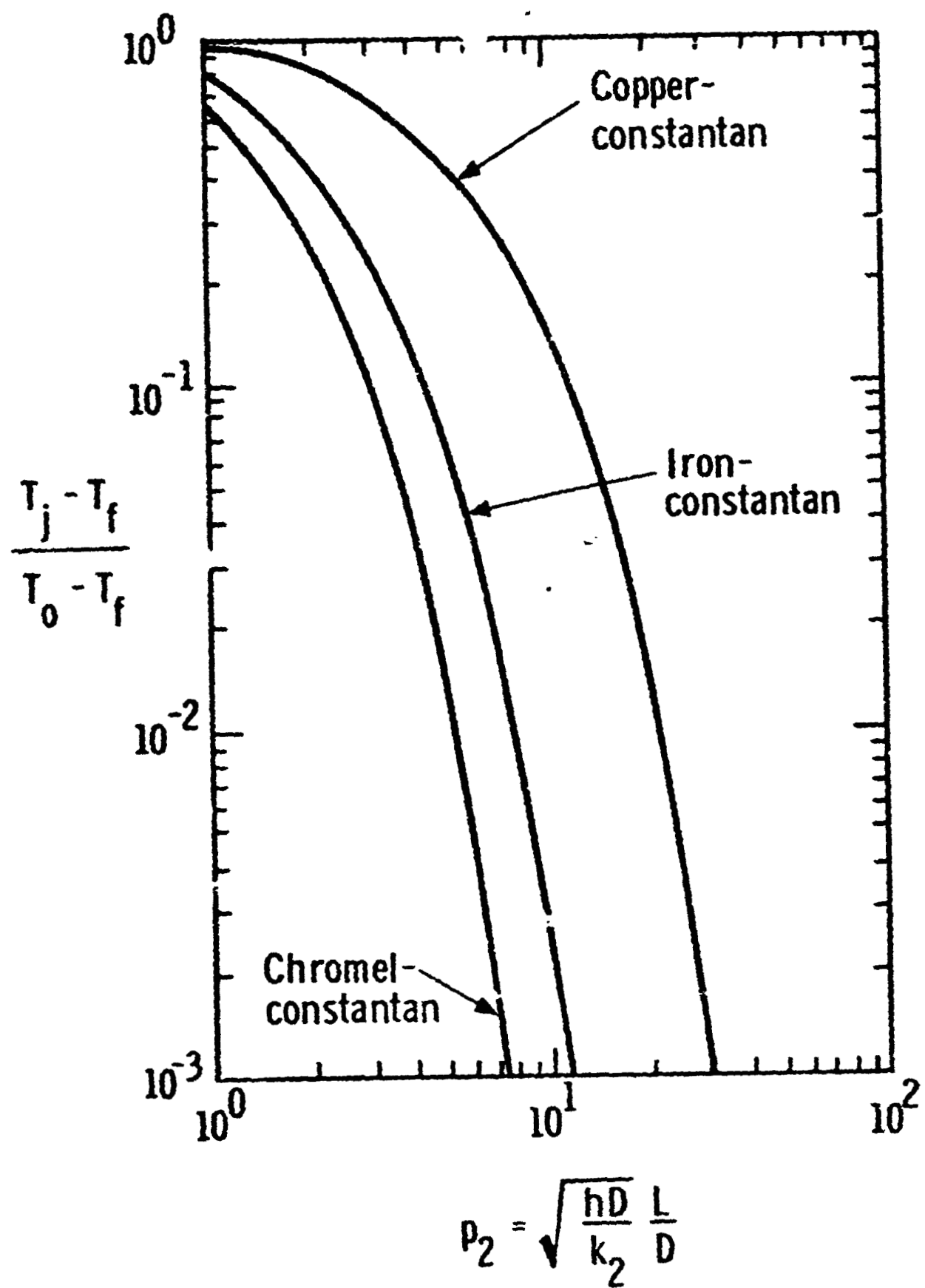


Figure 3-a. Comparison of three thermoelectric pairs, each with constantan as negative leg.

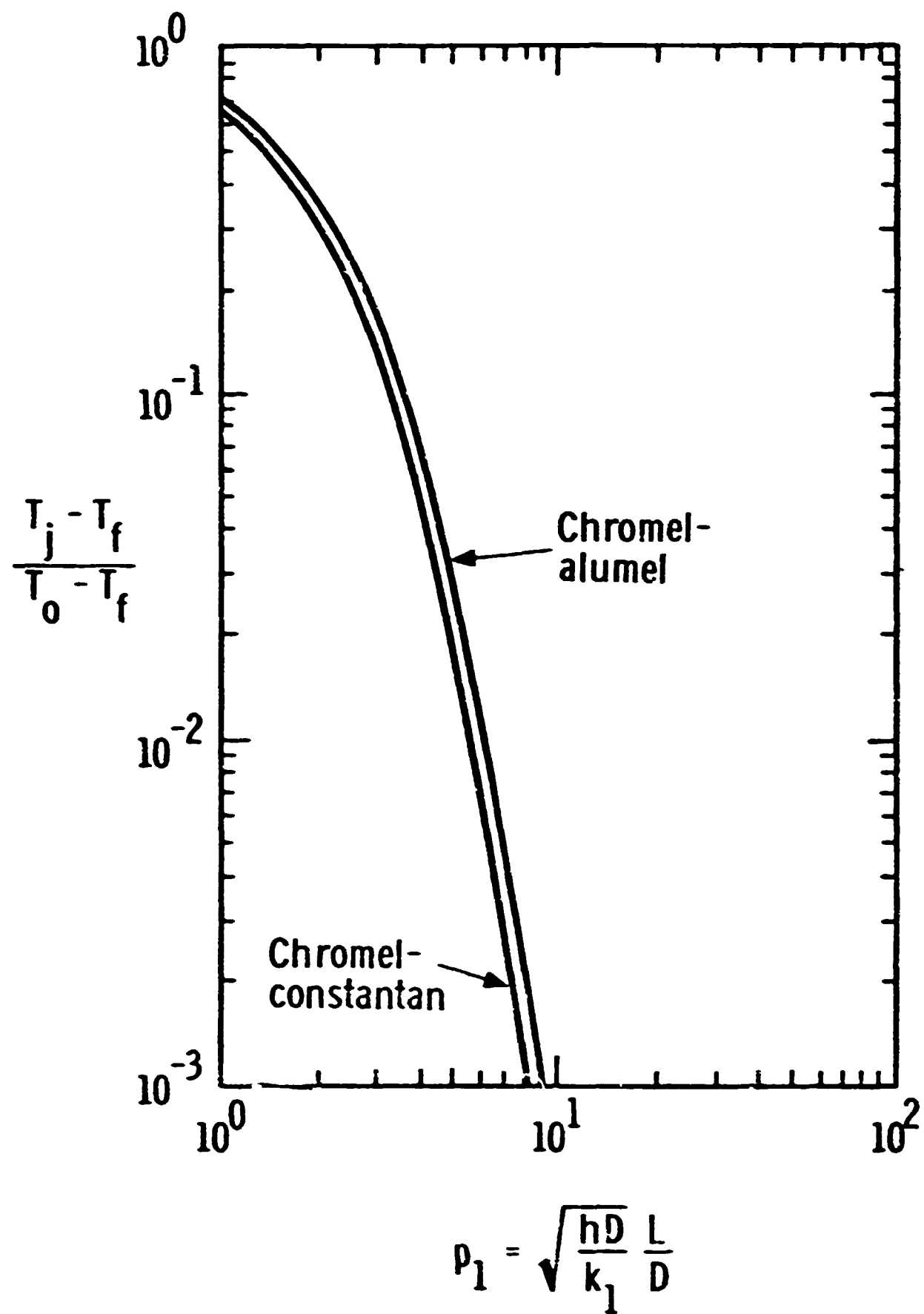
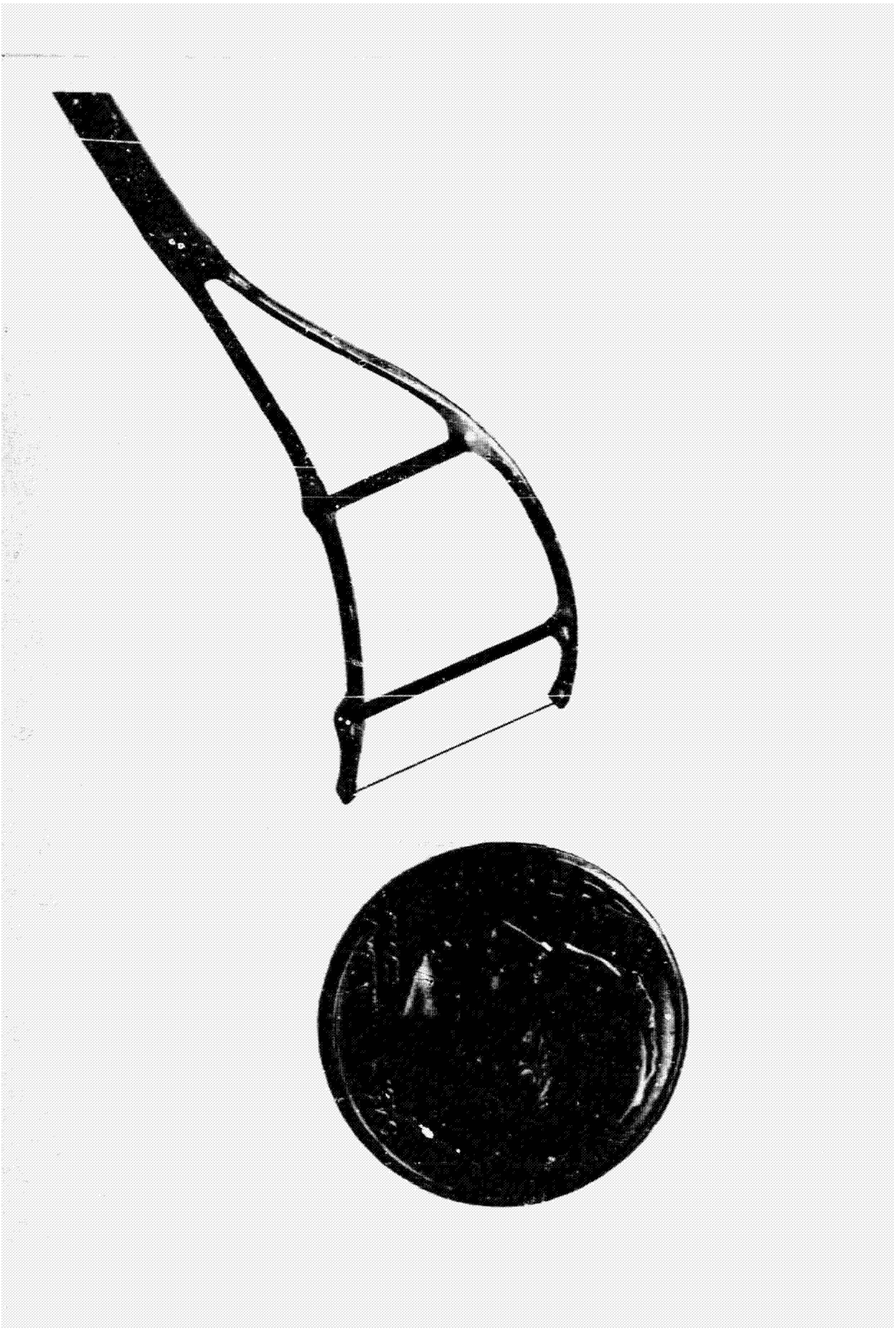


Figure 3-b. Comparison of two thermoelectric pairs, each with chromel as positive element.



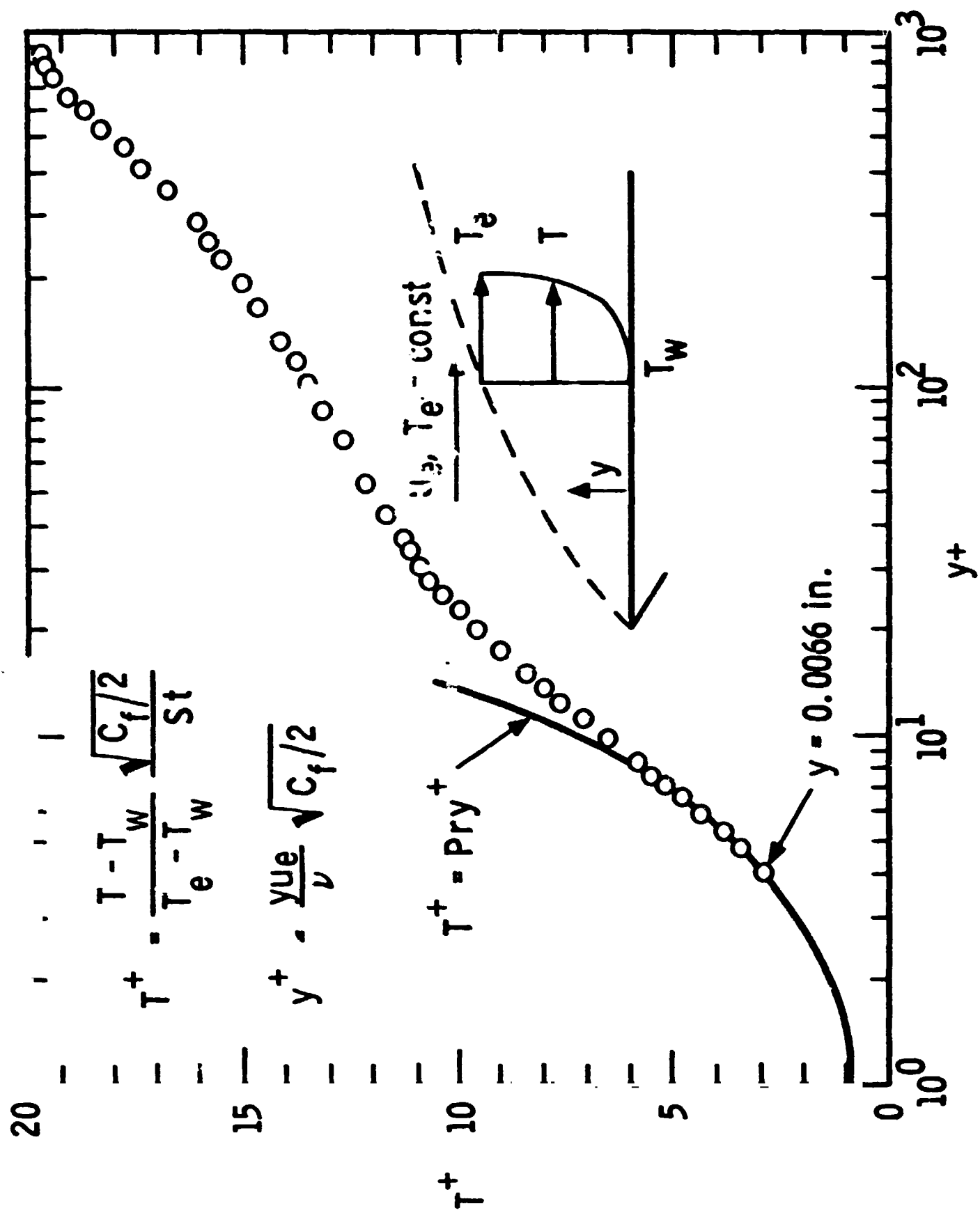


Figure 5. Comparison of experimental turbulent boundary-layer temperature data with laminar sub-layer equation.